Published online 28 July 2008

Nucleic Acids Research, 2008, Vol. 36, No. 15 ***5061–5073***
doi:10.1093/nar/gkn483

DNA organization by the apicoplast-targeted bacterial histone-like protein of *Plasmodium falciparum*

E. V. S. Raghu Ram[1], Rangeetha Naik[2], Munia Ganguli[2] and Saman Habib[1,*]

[1]Division of Molecular and Structural Biology, Central Drug Research Institute, Lucknow-226 001 and [2]Institute of Genomics and Integrative Biology, Delhi-110 007, India

Received March 4, 2008; Revised July 10, 2008; Accepted July 11, 2008

ABSTRACT

Apicomplexans, including the pathogens *Plasmodium* and *Toxoplasma*, carry a nonphotosynthetic plastid of secondary endosymbiotic origin called the apicoplast. The *P. falciparum* apicoplast contains a 35 kb, circular DNA genome with limited coding capacity that lacks genes encoding proteins for DNA organization and replication. We report identification of a nuclear-encoded bacterial histone-like protein (PfHU) involved in DNA compaction in the apicoplast. PfHU is associated with apicoplast DNA and is expressed throughout the parasite's intra-erythocytic cycle. The protein binds DNA in a sequence nonspecific manner with a minimum binding site length of ~27 bp and a K_d of ~63 nM and displays a preference for supercoiled DNA. PfHU is capable of condensing *Escherichia coli* nucleoids *in vivo* indicating its role in DNA compaction. The unique 42 aa C-terminal extension of PfHU influences its DNA condensation properties. In contrast to bacterial HUs that bend DNA, PfHU promotes concatenation of linear DNA and inhibits DNA circularization. Atomic Force Microscopic study of PfHU–DNA complexes shows protein concentration-dependent DNA stiffening, intermolecular bundling and formation of DNA bridges followed by assembly of condensed DNA networks. Our results provide the first functional characterization of an apicomplexan HU protein and provide additional evidence for red algal ancestry of the apicoplast.

INTRODUCTION

The apicoplast is the nonphotosynthetic plastid of apicomplexan parasites that include the genera *Plasmodium* and *Toxoplasma* and is believed to have arisen from a secondary endosymbiotic event involving an ancestral protist and an alga (1). The apicoplast is essential for parasite survival; it is the site for Type II fatty acid biosynthesis, nonmevalonate pathway of isoprenoid biosynthesis, and synthesis of heme intermediates within the parasite (2,3). Biochemical pathways operative within this organelle provide novel sites for drug intervention against malaria. Due to its essentially prokaryotic nature the processes of DNA replication, transcription and translation within the apicoplast are also validated drug targets (4–6).

Each sporozoan cell of *P. falciparum* carries a single apicoplast with apicoplast DNA (plDNA) copy number estimates varying from 1 to 15 (7,8). The ~35 kb, A + T-rich, circular double-stranded plDNA molecules of *P. falciparum* replicate via the D-loop/bi-directional *ori* mechanism at the late trophozoite-early schizont stage of the intraerythrocytic cycle. PlDNA replication origins (*ori*) localize within the inverted repeat (IR) region of the plDNA molecule (9–11). Although there is extensive sequence similarity between plDNA of *P. falciparum* and *T. gondii* they have distinct *in vivo* topology. The former is circular while the latter occurs as an oligomeric series of linear tandem arrays of the 35 kb genome. Light microscopy studies on *T. gondii* apicoplast genome have suggested that it is organized into a nucleoid that segregates into two equal portions during apicoplast division (8,12). The fact that a single plDNA circle is ~12 μm in circumference and several molecules have to be packed into an organelle with a diameter of only ~0.3 μm (8) as well as replicate and divide into daughter molecules without getting tangled is indicative of the involvement of a DNA-compacting protein in plDNA organization.

The apicoplast genome primarily encodes components of the transcription and translation machinery of the organelle (3,6) but lacks genes encoding any DNA organization or replication protein. Thus, all major protein

*To whom correspondence should be addressed. Tel: +91 522 2612411 to 418, ext. 4282; Fax: +91 522 2623405/2623938/2629504; Email: saman.habib@gmail.com; samamit@lycos.com

components involved in plDNA organization/replication must be nuclear-encoded and imported into the organelle. There is accumulating evidence on the components of the plDNA replication machinery. A ~220 kDa multi-domain polypeptide (PfPREX) that contains DNA polymerase as well as DNA primase, DNA helicase and 3′–5′ exonuclease activities (13) has been identified as a key enzyme for plDNA replication. Genes encoding putative apicoplast-targeted gyrase A and B have also been identified on Chr12 of *P. falciparum* and gyrase B has been functionally characterized (14,15). Ciprofloxacin and novobiocin, that target bacterial DNA gyrase, specifically inhibit replication of *P. falciparum* plDNA and also reduce parasite growth in culture (4,15) thus validating malarial apicoplast DNA replication as a drug target.

The dearth of information on proteins involved in organization of the *P. falciparum* apicoplast genome prompted us to investigate putative candidates from the parasite genome database. The prokaryotic nature and putative red algal origin of the apicoplast suggested the possible involvement of a histone-like protein ('heat unstable' or HU) (16) that is the primary organizational component of bacterial nucleoids, dinoflagellate chromosomes as well as red algal chloroplast genomes (17–19). A gene encoding a HU-ortholog that carries a conserved BHL domain (bacterial histone-like domain) together with a predicted N-terminal apicoplast targeting sequence was identified on Chr.9 of the *P. falciparum* nuclear genome. HU proteins are small basic proteins of prokaryotic origin that are structurally distinct from eukaryotic histones (20), belong to the DNABII family of DNA-binding proteins, and exhibit hetero- or homo-dimeric DNA binding. HU proteins also have regulatory effects on DNA replication, recombination and transcription (21–25). In bacteria, HU proteins together with the structurally related IHF (integration host factor), organize chromosomal DNA into periodic nucleosome-like structural units (26). Assuming an even distribution across the chromosome, *in vivo* concentrations of these proteins in *Escherichia coli* (27) provide for binding of one dimer only approximately every 125 bp, indicating that filament formation by HU could occur only locally (28). The presence of 10 other DNA-organization proteins such as histone-like nucleoid structuring protein (H-NS) and factor for inversion stimulation (Fis) that are also involved in DNA organization in *E. coli* (27) and their sequence preferences and co-operativity in binding DNA would further influence filament formation and condensation of *E. coli* DNA.

We report characterization of the *P. falciparum* nuclear-encoded bacterial histone-like protein (PfHU) and its interaction with apicoplast DNA. PfHU is expressed throughout the intra-erythrocytic phase of parasite growth, exhibits DNA binding and is capable of condensing DNA. The unique C-terminal domain of PfHU influences its interaction with DNA. Atomic Force Microscopic analysis shows that the protein is capable of forming both DNA bridges and bundles.

MATERIALS AND METHODS

Parasite culture

P. falciparum (strains 3D7 and NF54) was cultured in human RBCs maintained in RPMI-1640 supplemented with 0.5% AlbumaxII (Invitrogen). The parasites were synchronized with sorbitol (29).

Cloning, expression and purification of recombinant PfHU

The gene encoding the predicted 22.5 kDa *P. falciparum* bacterial histone-like protein (PlasmoDB ID PFI0230c) was amplified by PCR. DNA encoding unprocessed $PfHU_{up}$ (1–189 aa) was amplified using upstream (HU-f: 5′-CGCGGATCCTATGTAATATTATATTGTGTCC TT-3′) and downstream (HU-r: 5′-CGCGTCGACATAG ATTAACTTTTCATTTACATTTTC-3′) primers carrying BamHI and SalI sites, respectively with *P. falciparum* cDNA as template. The sequence encoding predicted processed PfHU ($PfHU_p$) (54–189 aa) was amplified using the forward primer HU-p (5′-CCGGGATCCATGTCACA GGCGATTACAAAG-3′) and HU-r as the reverse primer. Processed PfHU lacking 41 amino acids of the C-terminal end ($PfHU_{\Delta C}$) was amplified using HU-p as the forward primer and ΔHU-r (5′-CGCGTCGACCTT TATTAACTCCTTGAAAACTTTTG-3′) as the reverse primer. The fragments were cloned into pQE30 (Qiagen, USA) and sequenced to confirm their identity. Soluble recombinant $PfHU_{up}$, $PfHU_p$ and $PfHU_{\Delta C}$ proteins carrying the N-terminal RGS-6XHis tag were obtained after *E. coli* JM109 cells co-transformed with the RIG plasmid (gifted by Prof. W.G.J. Hol) were induced with 0.1 mM IPTG at 20°C for 18 h. The RIG plasmid carries tRNA genes whose transcripts recognize rare codons for the amino acids R, I and G in *P. falciparum* DNA expressed in *E. coli* (30). The recombinant proteins were purified on Ni-NTA Superflow (Qiagen, USA) and dialysed in a buffer containing 50 mM Tris–HCl (pH 7.6), 200 mM NaCl. $PfHU_p$ and $PfHU_{\Delta C}$ were further purified on a SP sepharose column. Final concentration of purified protein was determined by BCA assay. Far UV CD spectra analysis of purified $PfHU_p$ showed the presence of both α-helices and β-sheets and was comparable to other HU proteins thus indicating correct folding (data not shown). Chemical-crosslinking of $PfHU_p$ was carried out with 0.1% glutaraldehyde in 10 mM NaH_2PO_4 and 50 mM NaCl for 30 min at 37°C.

The gene encoding *Bacillus subtilis* HU (HBsu), was PCR-amplified from *B. subtilis* genomic DNA (upstream primer, 5′-CGGGGATCCATGAACAAAACAGAACT TATCAATG-3′ and downstream primer, 5′-CGTAAGC TTTTTTCCGGCAACTGCGTCTTTAAG-3′) and cloned in the pQE30 expression vector. The ~12 kDa recombinant protein carrying a N-terminal His-tag was purified by Ni-NTA chromatography and used as positive control in DNA circularization assays.

Antibody production, western blotting and immunoprecipitation

Antibodies against $PfHU_p$ were raised in rabbits and mice using purified $PfHU_p$. The titer of the raised antiserum was determined by ELISA.

For preparation of total parasite lysate, parasites were released by 0.05% saponin lysis, washed with PBS, and suspended in 1× SDS loading buffer containing protease inhibitors (Protease Arrest, GBiosciences, USA). After brief sonication, the cell lysate was separated on a 15% SDS–polyacrylamide gel. Western blotting was carried out (6) and the blot was developed using a chemiluminescent system (Amersham Biosciences, UK).

For immunoprecipitation, parasite cultures at 6–8% parasitaemia were harvested when cells were predominantly at the late trophozoite stage. Cells were washed with PBS and parasites were released by 0.05% saponin lysis. The parasite pellet was washed with PBS and lysed in chilled immunoprecipitation (IP) buffer (30 mM Tris–HCl pH 8.0, 300 mM NaCl, 1 mM EDTA, 1% v/v Triton X-100, 1% v/v Igepal and protease inhibitor cocktail) on ice for 30 min. After brief sonication, the lysate was centrifuged at 12 500 r.p.m. for 10 min. The supernatant was precleared by addition of 3 mg Protein A sepharose CL-4B for 1 h. The cleared supernatant was incubated with primary antibody (rabbit anti-$PfHU_p$ serum) for 2 h on ice with concomitant mixing. After centrifugation at 10 000 r.p.m. for 2 min at 4°C, the supernatant was incubated overnight with 5 mg Protein A sepharose at 4°C with continuous mixing. Sepharose beads were pelleted at 12 000 r.p.m. for 2 min at 4°C and washed five times with chilled IP buffer followed by two PBS washes. Immunoprecipitated proteins were obtained by treating the beads with nonreducing SDS lysis buffer. The sample was electrophoresed on a 15% gel and transferred onto a nitrocellulose membrane. The membrane was probed with mouse anti-HU_p serum as primary antibody and anti-mouse HRP conjugate as secondary antibody followed by development of the blot using a chemiluminescent detection system.

Electrophoretic mobility shift assay (EMSA)

Agarose gel electrophoresis was carried out with complexes of plasmid pBR322 and $PfHU_p$ or $PfHU_{\Delta C}$ as a function of protein concentration. Four hundred nanograms of supercoiled pBR322 (New England Biolabs, USA) or linear pBR322 DNA was used in the binding reaction with $PfHU_p$ or $PfHU_{\Delta C}$ in a reaction buffer containing 50 mM Tris–HCl pH 7.5, 0.1 mM EDTA. The reaction was incubated at 37°C for 40 min followed by electrophoresis on a 1% agarose gel at room temperature in 1× TAE buffer. The gel was stained with ethidium bromide (0.5 μg/ml) for 1 h, destained with 1× TAE and photographed.

For EMSAs on polyacrylamide gels, the binding reaction (20 μl) was carried out in 20 mM Tris–HCl, 0.1 mM EDTA and incubated for 30 min at room temperature. The gel was electrophoresed in 0.25× TBE. K_d determination was carried out by incubating 100 femtomoles of 5′-end-labeled 30 bp double-stranded oligo probe with increasing concentrations of protein as described in Ghosh and Grove (31). The region of a lane from the complex upto the free probe was taken as complex. K_d was calculated from the Hill equation, $f = f_{max} \times [PfHU_p]^n/(K_d + [PfHU_p]^n)$, where f is the fraction complex ($[PfHU_p]_b/[DNA]_t$), f_{max} is fraction complex at maximal saturation and $[PfHU_p]$ is protein concentration. The Hill coefficient (n) was set to one for single-site binding. Signals for bound and free probe were quantitated using OptiQuant1 software in Cyclone phosphorimager (Packard). K_d was calculated by curve-fitting using nonlinear regression in GraphPad PRISM software.

Supercoiling assay

Negatively supercoiled pBR322 (200 ng/reaction) was relaxed with 2 units of *E. coli* topoisomerase I (New England Biolabs, USA) in 10 mM Tris–HCl, pH 7.5, 50 mM NaCl, 10 mM $MgCl_2$, 0.1 mM EDTA and 100 μg/ml BSA for 2 h at 37°C. The relaxed DNA was incubated with increasing concentrations of $PfHU_p$ or $PfHU_{\Delta C}$ and the volume was adjusted with 1× dilution buffer (20 mM Tris–HCl, pH 7.5, 0.1 mM EDTA, 100 μg/ml BSA) and incubated for 1 h at 37°C. Reactions were terminated with proteinase K (0.5 μg/μl) and 0.5% SDS and incubated at 37°C for 1 h. The DNA was electrophoresed on 0.8% agarose gel in 0.5 × TBE for 14 h.

In vivo condensation assay

Escherichia coli JM109 cells co-transformed with pQE30-HU_p + RIG or the parent vector pQE30 + RIG as control were grown till the cultures reached an O.D. of 0.5. After induction with 0.5 mM IPTG for 3 h at 20°C, 1 ml culture was withdrawn and cells were washed twice with 1× TBS. Washed cells were suspended in 100 μl TBS, fixed with 0.5% glutaraldehyde and stained with 1.0 μg/ml DAPI for 30 min at 37°C. Cells were washed three times with 1× TBS and visualized in a fluorescence microscope (Leica DM5000B).

DNA-circularization assay

The ability of $PfHU_p$ to induce DNA circularization in the presence of T4 DNA ligase was assayed by incubating 2.5 ng of a 136 bp, ^{32}P 5′-end-labeled DNA probe with or without $PfHU_p$ (or $PfHU_{\Delta C}$) in a 20 μl reaction containing 1× ligase buffer at 25°C for 30 min. The 136 bp DNA was derived from a 369 bp PCR-amplified fragment from a *Mycobacterium* gene. The 369 bp fragment was digested with *Taq1* to give the 136 bp probe containing 5′ overhangs at both ends. The incubation of the DNA probe with PfHU was followed by addition of 4.5 U of T4 DNA ligase (Promega, USA) and further incubation at 22°C for 2 h. If samples were to be treated with BAL31 exonuclease (Fermentas, USA) after ligation, the ligation reaction was added to an equal volume of 2× nuclease buffer containing 1U of BAL31. The digestion reaction was incubated at 30°C for 15 min. The DNA was extracted

with phenol–chloroform, collected by ethanol precipitation and suspended in DNA loading dye. After electrophoresis on 7.5% 0.25× TBE-PA gel, the gel was dried and autoradiographed.

For the transformation assay, linear pBR322 (5 ng) was incubated with $PfHU_p$ and T4 DNA ligase as in the ligation assay above followed by protein removal by Proteinase K treatment (10 μg/reaction) and transformation of *E. coli* DH5α cells.

Chromatin immunoprecipitation

Chromatin immunoprecipitation (ChIP) assay was performed as described by Gissot *et al.* (32) with some modifications. Thirty milliliters of trophozoite stage *P. falciparum* culture was subjected to protein–DNA crosslinking using 1% (v/v) formaldehyde at 37°C for 15 min. Parasites were released by 0.05% saponin lysis and the parasite pellet was suspended in 1 ml ChIP buffer [30 mM Tris–HCl pH 8.0, 150 mM NaCl, 1 mM EDTA, 0.5% (v/v) Triton X-100 and 1% v/v Igepal]. Cells were incubated on ice for 20 min, sonicated nine times (Branson Digital Sonifier 450) at 30% amplitude for 10 s each with 1 min cooling between sonications. After centrifugation at 12 500 r.p.m. for 10 min at 4°C, the supernatant containing soluble chromatin was precleared with 50 μl of 50% Protein A sepharose CL-4B and 20 μg of sheared salmon sperm DNA for 2 h at 4°C. The beads were pelleted at 10 000 r.p.m. for 2 min. Preimmune serum or anti-$PfHU_p$ serum (1:75 dilution) was added to the supernatant and incubated at 4°C for 2 h. Forty microliters of 50% Protein A sepharose and 20 μg salmon sperm DNA was added to the mixture and incubated overnight at 4°C with continuous mixing. The sepharose beads were pelleted at 2000 r.p.m. at 4°C for 1 min and washed three times with ChIP buffer. This was followed by two washes with 1× TE and one wash with 1× TE and 0.01% SDS. Chromatin was eluted using 1× TE supplemented with 1% SDS. Chromatin was reverse cross-linked for 6 h at 65°C and treated with proteinase K (20 μg) for 2 h at 37°C. DNA was extracted with phenol–chloroform followed by ethanol precipitation. DNA from input and ChIP samples were resuspended in 100 and 20 μl TE, respectively. For PCR-amplification, 0.5 μl of input DNA and 2 μl of the ChIP sample were used as template. Primers for the nuclear gene *PfHU* and a plDNA sequence RIII (11) were used to amplify nuclear and apicoplast DNA, respectively. The PCR products were analysed on 1% agarose gel.

Confocal microscopy

P. falciparum cultures were processed for immunofluorescence labeling and confocal microscopy according to the method of Tonkin *et al.* (33). For mitochondrial labeling, live cells were incubated in 25 ng/ml MitoTracker Deep Red 633 (Molecular Probes) in PBS for 20 min at 4°C prior to fixation. Cells were washed with PBS and fixed in solution using 4% paraformaldehyde and 0.0075% glutaraldehyde in PBS for 30 min. After one wash with PBS, fixed cells were permeabilized with 0.1% Triton X-100 in PBS for 10 min. After another PBS wash, cells were treated with ~0.1 mg/ml sodium borohydride in PBS for 10 min. Cells were washed once with PBS, blocked in 3% BSA/PBS for 1 h and incubated overnight with rabbit anti-$PfHU_p$ serum (1:50 dilution in PBS containing 3% BSA) at 4°C. After three washes (10 min for each wash) with PBS, the cells were incubated with $AlexaFluor^{514}$-tagged anti-rabbit secondary antibody for 2 h at room temperature and allowed to settle onto coverslips coated with poly-L-lysine (100 μg/ml). The coverslips were then washed three times in PBS and mounted in anti-fade mounting media (Oncogene, USA). For apicoplast co-localization studies, the D10-ACP_{leader}-GFP line in which GFP is an apicoplast marker was used. Mouse anti-$PfHU_p$ Ab (1:25) or rabbit anti-GFP Ab (1 : 1000) (Molecular Probes) was used as primary antibody with Texas Red tagged anti-mouse Ab (Molecular Probes) or $Alexa\ Fluor^{488}$ tagged anti-rabbit Ab (Sigma) as secondary antibodies. The slides were viewed in a confocal laser-scanning microscope (Zeiss LSM 510) under a 63× oil immersion lens.

Atomic Force Microscopy (AFM)

Atomic force microscopy of DNA–PfHU complexes was carried out by using freshly cleaved mica treated with vapors of 3-aminopropyl triethoxysilane (APTES) at room temperature for 2 h for immobilization of samples (18). For sample preparation, $PfHU_p$ and linear pBR322 DNA were mixed at different dimer/bp ratios in 20 μl of AFM buffer (20 mM Tris–HCl, pH 7.5, 50 mM NaCl, 10 mM $MgCl_2$, 1 mM EDTA). The final concentration of DNA in the mix was ~1 ng/μl. After incubation for 10 min at room temperature, 10 μl of sample was dropped on APTES-coated mica and allowed to bind for 2 min at room temperature. The mica was washed extensively with deionized water, blotted at the edge and air-dried.

AFM imaging was carried out using the PicoSPM equipment (Molecular Imaging, AZ, USA). Images were obtained in the AAC mode with 225 μm long cantilevers that had resonance frequency of 65 kHz and force constant of 2.8 N/m. DNA contour length (in absence of protein) was calculated to be 1.403 μm (SD = 0.156 μm, $n = 95$), which is close to the expected contour length (1.439 μm) of the 4361 bp pBR322.

RESULTS

Structure modeling of PfHU reveals extensive fold conservation

The nuclear DNA-encoded 22.5 kDa *P. falciparum* protein (PlasmoDB ID PFI0230c) was identified as a candidate protein for DNA organization in the apicoplast due to the presence of a predicted bipartite apicoplast-targeting sequence that is the characteristic of nuclear-encoded proteins targeted to the organelle (34). The sequence has also been recently annotated as 'bacterial histone-like protein, putative' in the *Plasmodium* database (www.plasmodb.org). PfHU has a predicted 53 aa long signal and transit peptide with a high score in the apicoplast-targeting sequence prediction software Plasmo AP. This is followed by a conserved bacterial histone-like (BHL) domain found

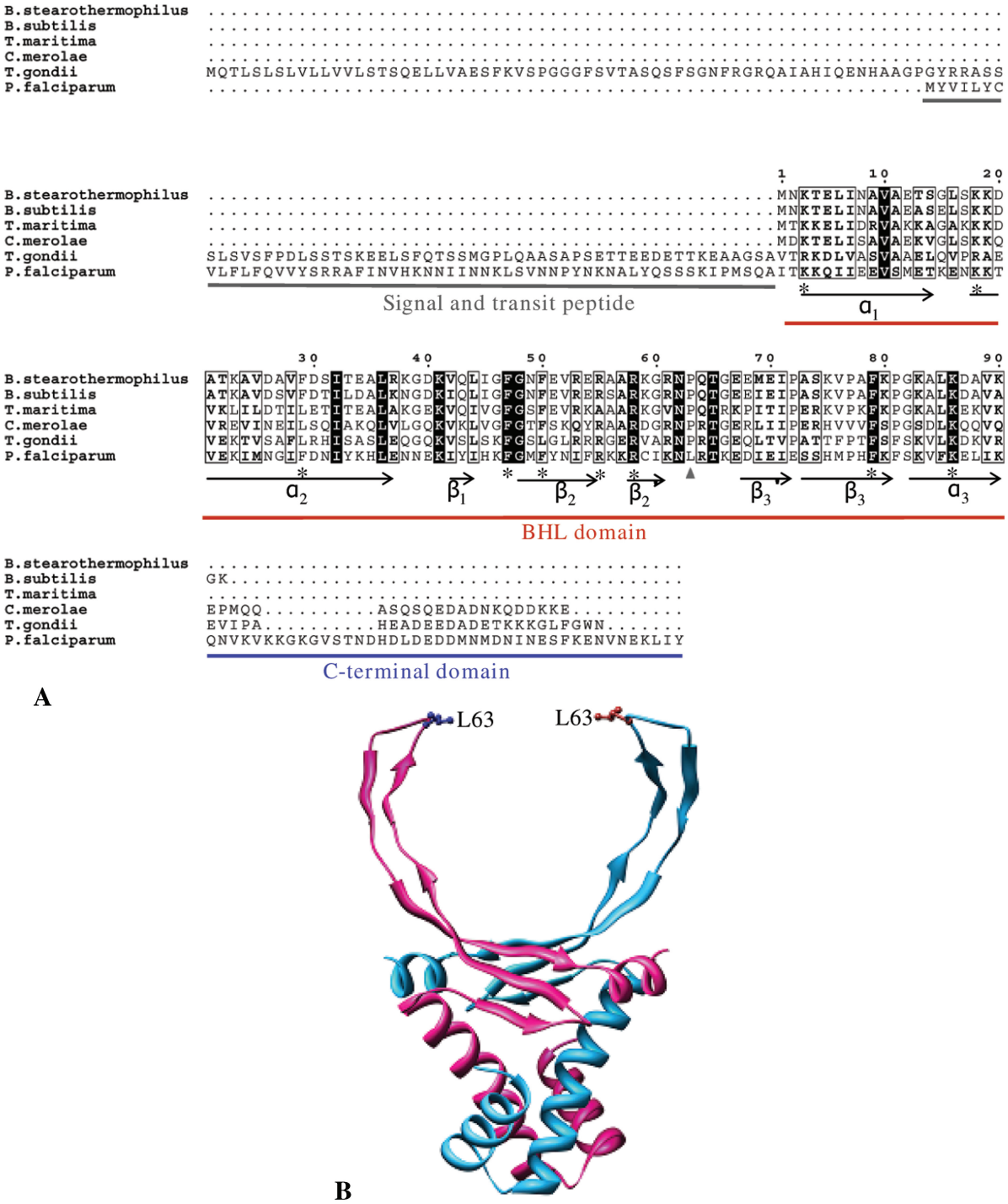

Figure 1. Sequence alignment and structure model of PfHU. (**A**) ClustalW alignment of PfHU with bacterial (*Bacillus stearothermophilus*, *B. subtilis*, *Thermotoga maritima*), red algal chloroplast (*Cyanidioschyzon merolae*) and apicomplexan (*Toxoplasma gondii*) HU proteins. Conserved residues described in the text are marked with asterisk. (**B**) Structure of the PfHU dimer modeled on the crystal structure of *B. stearothermophilus* HU. The position of the leucine residue (L63) that replaces the conserved proline of other HU proteins is indicated. The 42 aa C-terminal domain could not be modeled on any known protein structure and is not depicted in the figure.

in histone-like proteins in bacteria, dinoflagellates, red algal chloroplasts as well as in the related apicomplexan *T. gondii* (35) (Figure 1). PfHU also carries a 42 aa unconserved C-terminal extension beyond the BHL domain.

Alignment of the PfHU sequence with selected HU homologs from other organisms demonstrates significant sequence conservation within the BHL domain (Figure 1A) suggesting overall similarity of structure and function with other HU proteins. PfHU exhibits maximum homology with the *T. gondii* HU (30% identity) followed by the chloroplast HU of the red alga *Cyanidioschyzon merolae* (28% identity). Hydrophobic

residues in the BHL core, notably phenylalanine residues at positions 29, 47, 50 and 79, are conserved in PfHU. These residues are part of the dimerization signal and are involved in the formation of an aromatic hydrophobic core involving inter-subunit stacking (36,37). PfHU has an additional F54 residue that may also contribute to formation of the hydrophobic core. Structural analysis has shown that a number of arginine residues (R55, R58, R61) within the DNA-binding arms participate in hydrogen bonding or electrostatic contacts to the DNA (38). Of these, R55 and R58 are conserved in PfHU while R61 is replaced by a lysine. Surface-exposed lysine residues (K3, K18, K86) that line the body of the protein and have been shown to contribute to DNA binding (39) are also conserved in PfHU suggesting their contribution to wrapping of DNA around the protein.

Structure modeling of PfHU on the *Bacillus Stearothermophilus* structure (PDB ID: 1huu) (40) was carried out by SWISS-MODEL using the alignment mode. Extensive fold conservation in the PfHU BHL domain was revealed. The 42 aa C-terminal extension could not be modeled as it lacked significant homology with any known protein and contained regions of high disorder predicted using DisEMBL (41). The structure model of the PfHU homodimer is shown in Figure 1B. The predicted homodimer structure is comprised of a largely α-helical body with the α_1- and α_2-helices being formed by residue K3–T14 and K18–E37 of the predicted processed protein, respectively. β_1 (residue I42–I44), β_2 (residue G48–R55) and β_3 (residue S73–F81) strands form the saddle-like β sheet structure. β'_2 and β'_3 (R58–K61 and D68–E72, respectively) are part of the DNA-binding arm of PfHU. The DNA-binding arm of the PfHU monomer (residues 53–75) contains eight positively charged residues but lacks the highly conserved proline (P63) that is implicated in induction and/or stabilization of DNA bending by intercalating between base pairs (42). The DNA-binding arms of HU proteins have been described as disordered in crystal structures (36,43) and NMR studies show that the homodimer DNA-binding arms are folded at the tips and are flexible in solution (44).

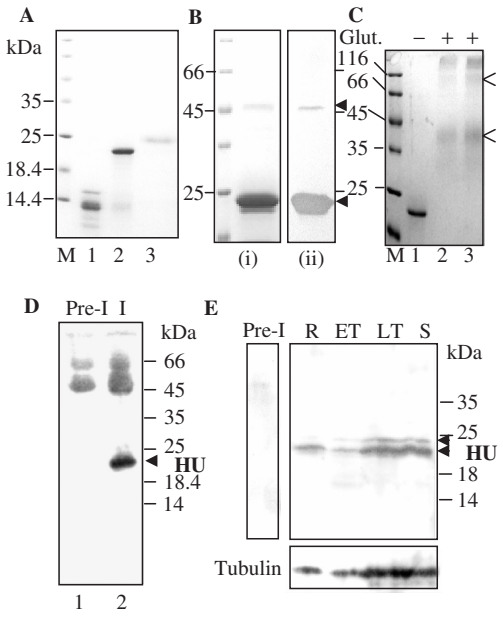

Figure 2. Expression of recombinant PfHU and its detection in *P. falciparum*. (**A**) Purified recombinant proteins $PfHU_{\Delta C}$ (lane 1), $PfHU_p$ (lane 2) and $PfHU_{up}$ (lane 3). M denotes marker lane. (**B**) Multimeric forms of purified $PfHU_p$ seen in Coomassie-stained SDS–PA gels (i) and detected by anti-6XHis antibody in Western blots (ii). (**C**) Chemical-crosslinking of 5 μg (lane 2) and 7 μg (lane 3) $PfHU_p$ indicates dimerization of the protein in solution. Glut., glutaraldehyde. Dimer and tetramer forms are indicated by arrows. (**D**) Detection of processed HU protein in *P. falciparum* lysates immunoprecipitated with rabbit anti-$PfHU_p$ antibody followed by detection using mouse anti-$PfHU_p$ antibody in a Western blot. Lane 1 represents immunoprecipitation with rabbit preimmune serum. (**E**) Expression of PfHU in *P. falciparum* intra-erythrocytic stages. The upper and lower panels are Western blots using anti-$PfHU_p$ antibody and α, β-tubulin antibodies (Sigma), respectively. R, rings; ET, early trophozoites; LT, late trophozoites; S, schizonts. Pre-I, lysate probed with preimmune serum. Arrows indicate unprocessed and processed forms of PfHU.

PfHU specifically binds apicoplast DNA

The processed form of PfHU ($PfHU_p$) was expressed as a soluble protein in *E. coli*. Although the expected size of the 6XHis-tagged processed protein is ~18 kDa, purified $PfHU_p$ ran at ~23 kDa on SDS–PA gels (Figure 2A) with the intact protein comprising ~93% of the purified fraction. The observed difference in size may be attributed to the presence of nonglobular domains in the protein or an excess of positively charged residues; such differences between expected and observed sizes on SDS–PA gels have also been observed for other *P. falciparum* proteins (15). The unprocessed form of PfHU ($PfHU_{up}$) carrying the apicoplast-targeting sequence was also expressed in *E. coli* and resolved at ~25 kDa on SDS–PA gels (Figure 2A). Purified recombinant processed PfHU lacking the 42 aa C-terminal domain ($PfHU_{\Delta C}$) ran at ~15 kDa, above its expected size of ~13 kDa, together with some truncated products. The truncated products were recognized by anti-His Ab in western blots (data not shown) indicating that they contain deletions from the C-terminal end. The major 13.5 kDa band would lack the α_3-helix in addition to the C-terminal domain but is likely to retain DNA binding. The two minor truncation products would additionally lack both the β_3 and β_3 strands and are thus unlikely to bind DNA. The 15 kDa band and its major truncated product of ~13.5 kDa that together comprised ~85% of the total purified protein are referred to as the 'C-terminal deletion' ($PfHU_{\Delta C}$) and were used for all calculations for quantitation of $PfHU_{\Delta C}$ for DNA-binding experiments.

When purified recombinant $PfHU_p$ was subjected to SDS–PAGE analysis, an additional band of ~44 kDa was observed together with the ~23 kDa monomeric form at high protein concentration (Figure 2B, i). The 44 kDa band corresponds to the size expected for the dimeric form of $PfHU_p$. Anti-His-antibody recognized the band in western blot confirming that it was the $PfHU_p$ dimer that either remained associated even after boiling in the presence of 0.1% SDS (Figure 2B, ii) or the $PfHU_p$ monomers reassociated in 0.1% SDS after removal from heat.

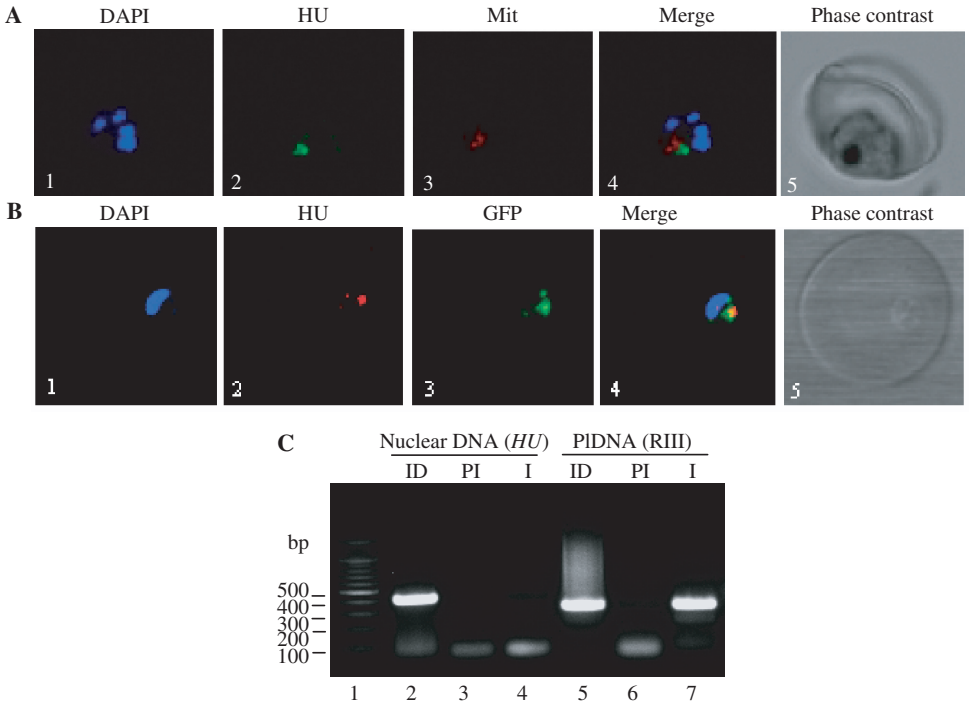

Figure 3. Localization of PfHU. (**A**) Immunolocalization of PfHU using confocal microscopy. Panels show nuclear DNA staining with DAPI (1), PfHU fluorescence (2), MitoTracker Red signal (3) and their overlap (4) in a late trophozoite. The corresponding phase–contrast scan is shown in (5). (**B**) Co-localization of PfHU and apicoplast-targeted GFP. Nuclear DNA stained with DAPI (1), PfHU signal (2), GFP signal (3) and their overlay (4) are shown. (**C**) Anti-$PfHU_p$ antibody specifically precipitates apicoplast DNA (plDNA) in a ChIP assay. Lanes 2–4 show PCR products obtained using primers for nuclear DNA (*HU* sequence) while lanes 5–7 show PCR products obtained using plDNA-specific primers for RIII. ID, input DNA; PI, preimmune serum; I, immune serum.

Treatment of purified $PfHU_p$ with 8 M urea caused dissociation of the dimer (data not shown) suggesting that hydrophobic interactions play a major role in dimerization of the protein *in vitro*. Glutaraldehyde-mediated crosslinking of $PfHU_p$ demonstrated that the protein existed predominantly as a dimer in solution (Figure 2C). A minor tetrameric form was also seen upon crosslinking.

Antibodies raised against recombinant $PfHU_p$ specifically recognized a ~22 kDa protein in western blots together with a fainter band at ~24 kDa (Figure 2E). This size difference corresponds to the difference observed for recombinant $PfHU_p$ and $PfHU_{up}$ indicating that the lower and upper bands represent processed and unprocessed forms of PfHU, respectively. Rabbit anti-$PfHU_p$ serum immunoprecipitated the processed form of PfHU that was specifically recognized by mouse anti-$PfHU_p$ serum (Figure 2D). A specific RT-PCR product of the length expected after cleavage of the single intron in the *PfHU* gene was also amplified from total parasite RNA (data not shown). These results confirm that *PfHU* is translated in the parasite. PfHU was also detected in parasite lysates from synchronized cells at different intra-erythrocytic stages (Figure 2E). Expression of the protein was observed at all stages and comparison with parasite tubulin levels indicated constitutive PfHU expression during the *P. falciparum* erythrocytic cycle.

P. falciparum carries three DNA genomes- nuclear, apicoplast and mitochondrial (45). To address the possibility of PfHU also serving as a mitochondrial/nuclear DNA organization protein, we carried out immunofluorescence detection of PfHU using anti-$PfHU_p$ antibody in confocal microscopy. PfHU localized to an organellar structure close to, but distinct from, the mitochondria stained with Mitotracker Red (Figure 3A). PfHU signal was also not observed in nuclei that were stained with DAPI. Additionally, PfHU co-localized with apicoplast-targeted GFP in the D10 ACP_{leader}-GFP line with GFP as an apicoplast marker (Figure 3B). These data confirm apicoplast-specific localization of PfHU in *P. falciparum* as also reported for the HU protein of *T. gondii* (46). In order to investigate whether PfHU interacts with *P. falciparum* apicoplast DNA *in vivo*, we carried out chromatin immunoprecipitation (ChIP) of total *P. falciparum* DNA using anti-$PfHU_p$ antibody. This was followed by PCR-amplification of immunoprecipitated DNA using primer pairs for amplification of a 411 bp internal region of the *PfHU* gene representing nuclear DNA and a 332 bp fragment (RIII) (11) representing the apicoplast genome. While both primer pairs amplified the corresponding fragments from input DNA (Figure 3C, lanes 2 and 5), amplification of only the apicoplast-specific fragment was observed when DNA precipitated with the anti-$PfHU_p$ immune serum was used as template (lane 7). Neither fragment was amplified from DNA immunoprecipitated using preimmune serum (lanes 3 and 6). The clear recovery of apicoplast DNA in the ChIP assay indicated that PfHU binds specifically to the apicoplast genome thus

strengthening its candidature as a key protein in plDNA organization.

$PfHU_p$ binds and condenses DNA

The DNA-binding activity of recombinant $PfHU_p$ was investigated by electrophoretic mobility shift assays (EMSAs) in agarose gels using supercoiled and linear pBR322. The mobility of the supercoiled form was retarded sharply by $PfHU_p$ starting at the protein/DNA mass ratio of 0.5 while retardation of linear DNA was clearly visible only beyond the protein/DNA mass ratio of 2 (Figure 4A). This indicated that $PfHU_p$ exhibits preferential condensation of supercoiled DNA compared to linear DNA. EMSA with increasing concentrations of $PfHU_p$ and $PfHU_{\Delta C}$ incubated with supercoiled pBR322 (Figure 4B) revealed a difference in their DNA condensing properties. While $PfHU_p$ condensed DNA *in vitro* at a concentration of 8 μM (protein/DNA mass ratio ≥10) when nearly all the DNA was retained in the well, complete condensation of DNA by $PfHU_{\Delta C}$ was observed at 6 μM (protein/DNA mass ratio = 6.2). Additionally, in contrast to $PfHU_p$, no intermediate retardation forms were observed with $PfHU_{\Delta C}$. A minor retardation with 2 μM $PfHU_{\Delta C}$ was followed by complete condensation of DNA as the protein was increased from 4 to 6 μM. These results indicate a role of the 42 aa C-terminal domain in influencing the DNA-condensation properties of $PfHU_p$.

The effect of salt on DNA–protein interaction was assayed by addition of 50 or 100 mM NaCl to the binding reaction at different PfHU/DNA mass ratios. Partial inhibition of binding was observed with 50 mM NaCl as a much greater amount of $PfHU_p$ was required to cause the same level of retardation (Figure 4C). Binding was completely inhibited by 100 mM NaCl and no retardation was observed even at the protein/DNA mass ratio of 10 indicating that interaction between $PfHU_p$ and DNA was primarily electrostatic.

The effect of increasing concentrations of $PfHU_p$ and $PfHU_{\Delta C}$ on DNA supercoiling (Figure 4D) showed that the supercoiling ability of both the products was negligible. This contrasts with reports for other HU proteins (47) that hinder relaxation by topoisomerase I and constrain negative supercoils in a concentration-dependent manner.

The effect of over-expression of $PfHU_p$ on *E. coli* DNA was examined by fluorescence microscopy of DAPI-stained *E. coli* cells that were transformed with the expression vector pQE30 or the $PfHU_p$ expression vector pQE30-HU_p + RIG plasmid and induced with IPTG (RIG overcomes codon bias for expression of *P. falciparum* genes in *E. coli*). Compared with control cells, cells expressing $PfHU_p$ exhibited very slow growth upto 3 h after induction. Additionally, control cells lacking $PfHU_p$ exhibited uniform DNA distribution while extensive condensation of the *E. coli* nucleoid was visible in cells expressing $PfHU_p$ (Figure 5). This result indicates that an excess of $PfHU_p$ causes greater compaction of *E. coli* nucleoids. Similar compaction of *E. coli* nucleoids was also observed with overexpression of $PfHU_{\Delta C}$ (data not shown).

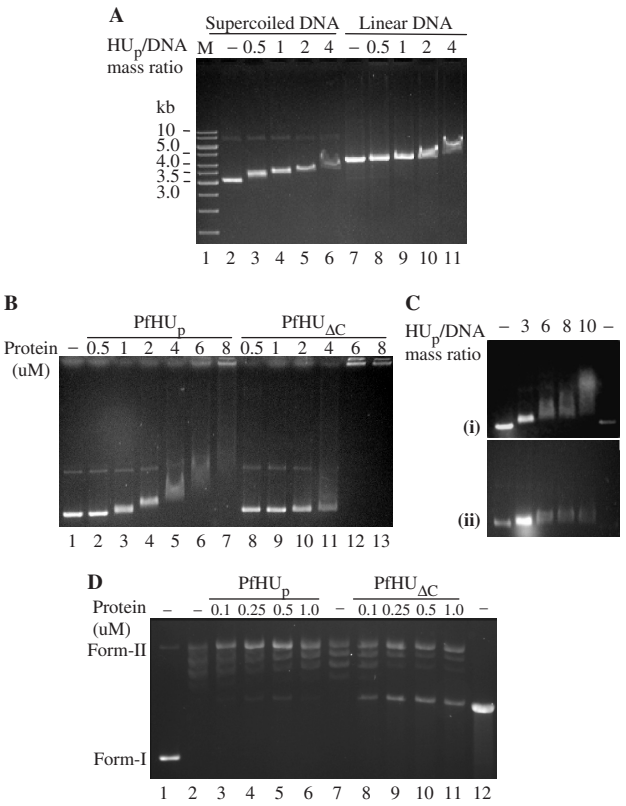

Figure 4. DNA-binding properties of $PfHU_p$. (**A**) EMSA depicting binding of $PfHU_p$ to supercoiled and linear pBR322. Four hundred nanograms of supercoiled (lanes 2–6) or linear (lanes 7–11) plasmid was incubated with $PfHU_p$ at different protein/DNA mass ratios. M, DNA marker. (**B**) EMSA with increasing concentrations of $PfHU_p$ (lanes 2–7) and $PfHU_{\Delta C}$ (lanes 8–13) using supercoiled pBR322 DNA. Lane 1 is free DNA. (**C**) Binding of $PfHU_p$ to supercoiled DNA in the presence of 50 mM (i) and 100 mM (ii) NaCl. (**D**) DNA supercoiling assay with increasing concentrations of $PfHU_p$ (lanes 3–7) and $PfHU_{\Delta C}$ (lanes 8–12). Lane 1 is naked DNA (negatively supercoiled pBR322), lane 2 is pBR322 partially relaxed with topoisomerase I, lane 12 is linearized pBR322. Form-I, supercoiled DNA; form-II, relaxed DNA.

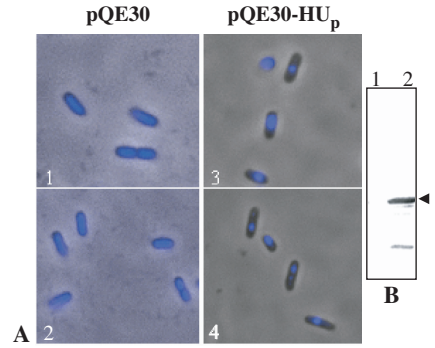

Figure 5. $PfHU_p$-mediated condensation of *E. coli* nucleoids. (**A**) Fluorescence images of DAPI-stained, IPTG-induced *E. coli* cells that had been co-transformed with pQE30 + RIG plasmid (1 and 2) or pQE30-HU_p + RIG plasmid (3 and 4). (**B**) Western blot using anti-$PfHU_p$ antibody to detect expression of $PfHU_p$ in *E. coli* cells co-transformed with RIG and pQE30 (lane 1) or pQE30-HU_p (lane 2) followed by induction with IPTG. Arrow indicates the $PfHU_p$ band.

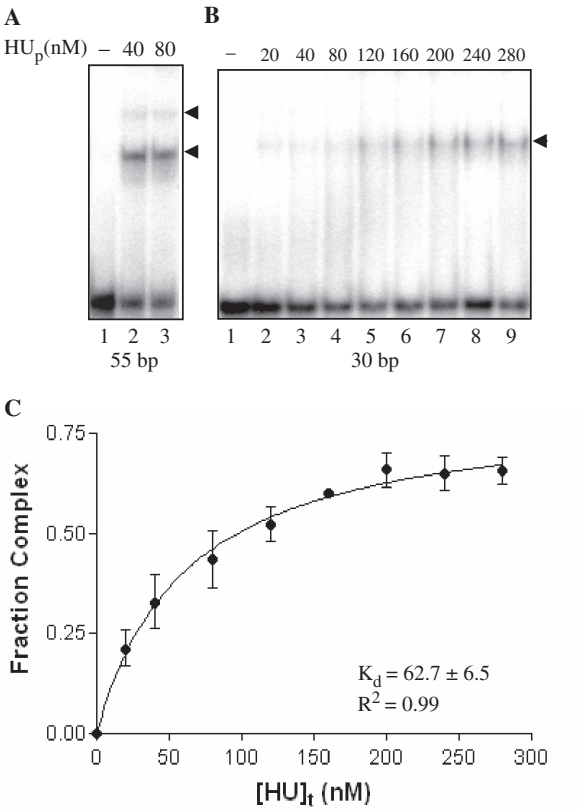

Figure 6. Binding site length and affinity of $PfHU_p$ for DNA. (**A**) EMSA showing binding of $PfHU_p$ with end-labeled 55 bp probe. (**B**) EMSA of $PfHU_p$ with a 30 bp probe. (**C**) The K_d of the single complex obtained in (B) was determined from its binding isotherm by curve-fitting using nonlinear regression. The mean K_d value from three repeat experiments was estimated as 62.7 ± 6.5 nM.

The minimal binding-site length of PfHU was determined by using double-stranded oligonucleotide probes of 23, 30 and 55 bp in binding reactions resolved in EMSAs on PA gels. A very faint smeared complex was observed with the 23 bp probe (data not shown) while a single clear complex was obtained with the 30 bp probe (Figure 6B). Two complexes were obtained when the 55 bp probe was used (Figure 6A) indicating a binding site of between 24 and 27 bp. The 55 bp probe containing two $PfHU_p$ dimer binding sites was also used to determine the active fraction of $PfHU_p$ by titrating 125 nM of $PfHU_p$ dimer with increasing concentrations (2.5–160 nM) of the 55 bp DNA probe in EMSA (data not shown). The protein saturated at ~60 nM DNA indicating that >95% of the protein was active. The affinity of the $PfHU_p$ dimer for DNA was determined by calculation of K_d of the single complex obtained with the 30 bp probe (Figure 6C). The K_d value obtained for $PfHU_p$ was 62.7 ± 6.5 nM.

$PfHU_p$ promotes DNA concatenation

Bacterial HU is capable of mediating DNA ring closure (48) while its dinoflagellate counterpart promotes concatenation of DNA fragments and inhibits DNA circularization (18). The ability of $PfHU_p$ to promote circularization of short-length DNA fragments as a result of

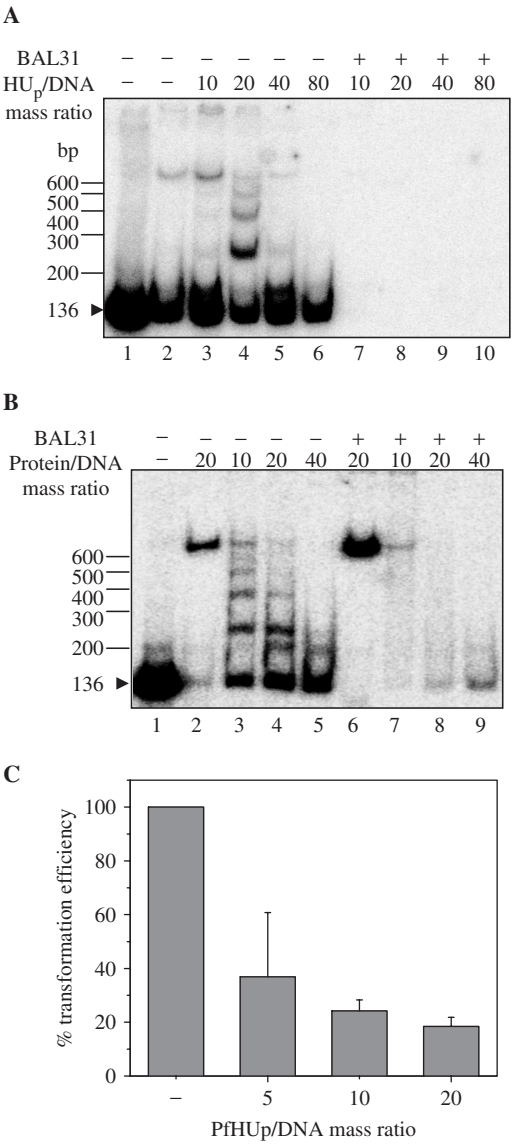

Figure 7. DNA concatenation by $PfHU_p$. (**A**) DNA ligation of a 136 bp labeled DNA fragment carried out in the presence of increasing concentrations of $PfHU_p$ (lanes 3–6). Lane 1 is free DNA while lane 2 is DNA probe ligated in the absence of $PfHU_p$. Ligation reactions were treated with BAL31 nuclease to detect circularized DNA products (lanes 7–10). (**B**) Ligation of the 136 bp fragment in the presence of increasing concentrations of $PfHU_{\Delta C}$ (lanes 3–5 and 7–9). Lane 1 is free DNA while lanes 2 and 6 are DNA probe ligated in the presence of HBsu as positive control for DNA circularization. (**C**) Percentage transformation efficiency of ligation reactions of linear pBR322 carried out in the presence of $PfHU_p$. Transformation efficiency was calculated as percentage of that obtained with pBR322 ligated in the absence of $PfHU_p$. Mean and SE of repeat determinations is plotted.

protein-mediated DNA bending was tested in a T4 ligase-mediated DNA ligation assay. Ligation of a 136 bp DNA fragment was carried out in the presence of increasing concentrations of $PfHU_p$ and $PfHU_{\Delta C}$ (Figure 7A and B). HBsu (*B. subtilis* encoded HU homolog) was included as positive control for cyclization (49). The ligation products were also treated with exonuclease to identify exonuclease-resistant circularized DNA. Unlike bacterial HU and similar to the dinoflagellate HCc3,

$PfHU_p$ promoted concatenation of DNA as evident from the increase in exonuclease-sensitive linear multimers of the 136 bp DNA fragment upto $PfHU_p$/DNA mass ratio of 20 (Figure 7A). Higher concentrations of protein ($PfHU_p$/DNA mass ratio of 40 and 80) inhibited concatenation. Similar results were obtained with $PfHU_{\Delta C}$ indicating that the C-terminal extension was not responsible for mediating DNA concatenation (Figure 7B). $PfHU_p$ and $PfHU_{\Delta C}$ also promoted concatenation and inhibited circularization of a longer 207 bp DNA fragment in a concentration-dependent manner (data not shown).

$PfHU_p$ also inhibited DNA circularization as evident from results of the transformation assay (Figure 7C) where linear pBR322 (5 ng) was incubated with $PfHU_p$ and T4 DNA ligase as in the ligation assay above followed by transformation of *E. coli* DH5α cells. $PfHU_p$ exhibited dose-dependent inhibition of DNA circularization. Upto 80% inhibition was observed at $PfHU_p$/DNA mass ratio of 20, which corresponds to the protein concentration at which maximum concatenation is seen in Figure 7A.

AFM studies

Atomic Force Microscopy of $PfHU_p$–DNA complexes at different $PfHU_p$-dimer/bp ratios provided further evidence for DNA condensation mediated by $PfHU_p$ (Figure 8). At lower concentration of protein (dimer/bp ratio 1 : 750) stiffening of DNA strands was evident (Figure 8B, i). Intermolecular DNA bundling with two DNA strands forming a tight bundle was also observed at this concentration (Figure 8B, ii). $PfHU_p$-mediated formation of DNA loops (Figure 8C, ii) was seen at the dimer/bp ratio of 1 : 500 and assembly of condensed DNA complexes with a small number of foci and extruding DNA loops was initiated (Figure 8C, i and iii). This data indicated that $PfHU_p$ also forms DNA bridges. Formation of larger $PfHU_p$–DNA complexes was seen at higher protein concentration (dimer/bp ratio 1 : 250) (Figure 8D). These complexes appeared to be formed by the assembly of large DNA bundles/bridges brought together by intermolecular interactions between $PfHU_p$ subunits (Figure 8D, ii and iii).

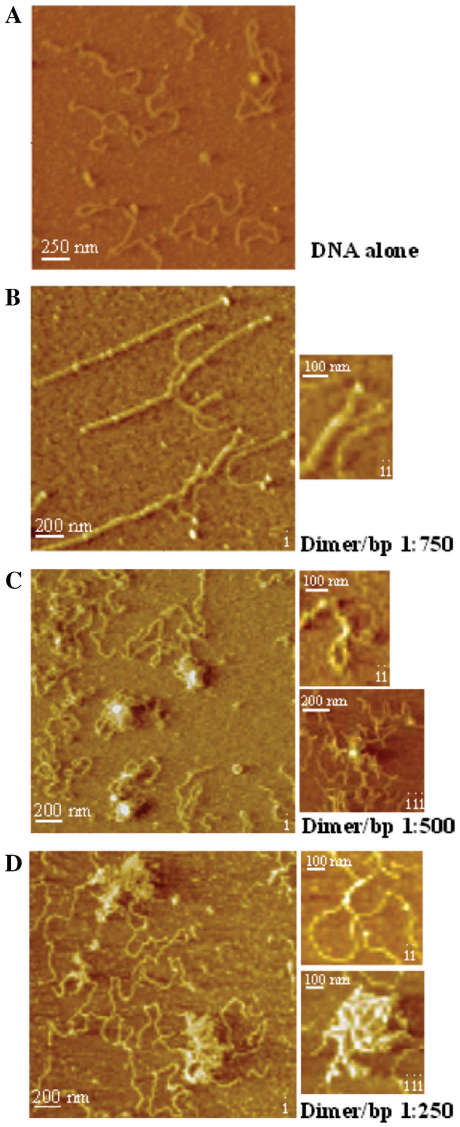

Figure 8. AFM images of $PfHU_p$-linear pBR322 DNA complexes with increasing dimer/bp ratio. (**A**) DNA in the absence of protein. (**B**) Dimer/bp ratio of 1 : 750. Stiffened DNA strands (i) as well as DNA bundles (ii) are shown. (**C**) Dimer/bp ratio of 1 : 500. Formation of complexes with a small number of foci and extruding DNA loops (i), a DNA bridge resulting in DNA looping (ii) and a nucleoprotein complex with a single focus (iii) are shown. (**D**) Dimer/bp ratio of 1 : 250. Large complexes (i and iii) are formed by the assembly of DNA bundles (ii) and bridges.

DISCUSSION

Proteins that mediate organization of the *Plasmodium* organellar genomes are yet to be identified and functionally characterized. While core histones (H2A, H2B, H3 and H4) for nuclear DNA assembly are encoded in the genome together with a few histone variants (50), two nucleosome assembly proteins, PfNAPS and PfNAPL, which preferentially interact with H3–H4 tetramer histones have also been characterized (51). Although the high mobility group (HMG) protein Abf2 is an abundant basic protein that supercoils mitochondrial DNA in yeast (52), the HMG homologs on the *P. falciparum* genome lack predicted mitochondrial-targeting signals. On the other hand, a mitochondrial-targeting sequence is predicted for a putative histone 2B (PF11_0062) encoded by the nuclear genome. Of the 517 nuclear-encoded proteins predicted to target to the apicoplast, PfHU (PFI0230c) is the only one with a dsDNA-binding BHL domain similar to HU-like DNA organization proteins of plastids. Our results identify PfHU as a component of the apicoplast and confirm its interaction with apicoplast DNA. The DNA-binding characteristics of PfHU and its effect on bacterial nucleoid condensation are also indicative of its role as a plDNA architecture protein in *P. falciparum*.

Sequence-function analyses of PfHU reveal some interesting features. While the DNA-intercalating proline (P63) and surrounding residues are conserved in most HU proteins, a few exceptions such as bacteriophage SPO1–encoded TF1 and HU from *Thermotoga*, *Thermus*, *Aquifex*, *Deinococcus* and *Mycoplasma* have R61 replaced

by V or M residues (53). R61 is replaced by a K residue in *P. falciparum* while the P63 residue is replaced by L, thus converting the conserved HU RNP motif into a KNL motif. These observed substitutions may be explained by the low G + C content (~75% A + T) of the *P. falciparum* genome which results in a bias against residues G, P, A and R. Significantly, the *T. gondii* HU sequence (*T. gondii* genome has 47% A + T) retains conserved R61 and P63 residues. P63 is implicated in induction and/or stabilization of DNA bending and the absence of this residue in PfHU may explain the inability of the protein to induce DNA circularization. An alternative possibility is that PfHU may bend DNA, but association of multiple PfHU molecules results in out-of-phase bending. HCc3, a likely constituent of permanently condensed crystalline chromosomes of the dinoflagellate *Crypthecodinium cohnii*, also lacks P63 and fails to induce DNA circularization *in vitro*; similar to PfHU, HCc3 promotes DNA concatenation (18). Assaying DNA circularization by PfHU after mutagenesis to restore P63 would be required to confirm the role of L63 in preventing DNA bending by the protein. Analysis of the αP64L mutant of IHF (position corresponding to P63 in HU) that interacts with DNA in a site-specific manner has demonstrated that the substitution affects binding specificity of the protein (54,55).

As opposed to other HU proteins, $PfHU_p$ is unable to constrain negative supercoils. The P63 residues in the *E. coli* HU dimer intercalate into the minor groove of DNA 9 bp apart and induce two DNA kinks. These kinks are not co-planar and result in negative supercoiling (underwinding) of ~31° per bp (56). The observed absence of DNA-bending activity of PfHU offers an explanation for its inability to constrain negative supercoils in the DNA double-helix.

HU proteins bind to random DNA sequences with K_d values ranging from 5 to 2500 nM with *E. coli* HU exhibiting a K_d value of ~200–300 nM (53,57). The K_d value of PfHU–DNA interaction is ~63 nM indicating slightly higher affinity of the protein for DNA compared to *E. coli* HU. HU proteins have been reported to interact with DNA with binding sites of between 9 and 42 bp (57). It has been suggested that variations in HU-binding site lengths are determined by the presence or absence of amino acids capable of forming salt bridges distal to sites of kinking (58). In HU homologs with shorter binding sites, K3 is proposed to form a salt bridge with D26. In TF1, which lacks D26, K3 contacts DNA 8–9 bp away from the DNA kink leading to a longer binding site of 37 bp. Similarly, the absence of D26 in PfHU may explain its binding site length of 24–27 bp.

There is a difference in patterns of DNA shifts obtained with increasing concentrations of $PfHU_p$ and $PfHU_{\Delta C}$, with sudden transition to highly condensed DNA observed with the latter. The 42 aa C-terminal domain present in $PfHU_p$ has a predominance of acidic residues (net PI of $PfHU_p$ is 8.81). $PfHU_{\Delta C}$, which lacks the domain, has a PI of ~9.5. The DNA shifts observed in EMSAs with the two proteins indicate that rapid condensation of DNA follows an initial 'nucleation' step with increasing $PfHU_{\Delta C}$/DNA ratio, while stepwise assembly of intermediate forms is observed with the full-length $PfHU_p$. Although the precise mode for this is unclear, the negatively charged C-terminal domain unique to $PfHU_p$ may directly influence interaction of the protein with DNA. Alternatively, rapid DNA condensation by $PfHU_{\Delta C}$ may be caused by enhanced cooperativity of binding of $PfHU_{\Delta C}$ dimers to DNA and/or increased intramolecular attraction between $PfHU_{\Delta C}$ dimers bound at different sites on DNA. The C-terminal domain also seems to influence stability of $PfHU_p$ as removal of the domain results in greater protease-sensitivity. *In vivo*, the intrinsically unstructured C-terminal domain may interact with other parasite proteins (59) and influence PfHU activity.

AFM analysis of DNA–protein complexes formed with $PfHU_p$ showed formation of DNA bundles and bridges. DNA bundling is a property exhibited by the RecA protein (60) and also reported for the dinoflagellate HCc3 (18). DNA bundling by $PfHU_p$ may bring the ends of two or more DNA strands closer thus promoting ligase-mediated concatenation observed with $PfHU_p$. The bundling of two strands would be mediated by the interaction between two $PfHU_p$ dimers, each of which binds to a single DNA strand. Indeed, formation of such tetrameric $PfHU_p$ forms is indicated by chemical-crosslinking of the protein in solution. The clustering of long DNA bundles and bridges to form large complexes observed at high $PfHU_p$ concentration could be mediated by intermolecular interactions between $PfHU_p$ tetramers. Thick rigid DNA–protein filaments as observed for high concentrations of *E. coli* HU (1 dimer per 1.8 bp) (28) are seen at much lower concentrations of $PfHU_p$ (1 dimer per 750 bp). Unlike *E. coli* HU, whose AFM analysis shows DNA bending mediated by single dimers at one dimer per 92 bp (28), DNA bending was not observed with $PfHU_p$ consistent with our observation of inhibition of DNA circularization with the protein. DNA stiffening and bundling by $PfHU_p$ may explain the inhibition of circularization observed with the protein. DNA loop formation and bridging by $PfHU_p$ is also clearly seen in AFM images. Formation of DNA bridges by the bacterial nucleoid structuring protein, H-NS, which is structurally distinct from HU, has been reported (61). DNA bridging resulting in formation of loops may have implications not only in DNA compaction mediated by $PfHU_p$ but also suggests a possible mechanism by which it may influence transcription processes in the apicoplast.

The origin of apicomplexan plastids has been of recent interest and their rhodophyte versus chlorophyte ancestry has been debated (62,63). The presence of a functional HU-like protein in apicomplexan plastids provides further support for red algal ancestry of the apicoplast; HU-like proteins are found in plastid genomes of red algal lineage but not in those of green alga (64). Additionally, the sequence of PfHU is closest to red algal plastid HUs of *C. merolae* and *Guillardia theta* and the apicomplexan and red algal HUs cluster with cyanobacteria HUs (35,65). The presence of a nuclear gene encoding apicoplast-targeted HU in *P. falciparum* indicates that the gene was acquired by a secondary endosymbiotic event from a red alga with subsequent transfer from the red algal plastid to the host nuclear genome.

Our results provide evidence for the involvement of a HU-like protein in DNA organization and compaction in the plastid of an apicomplexan. Apart from being major components of nucleoids, HU proteins in bacteria also play important roles in initiation of DNA replication and regulation of transcription (21,24,66). Although the specific roles that HU may play in apicoplast DNA replication and/or regulation of transcription remain to be elucidated, the reported missegregation of the *T. gondii* apicoplast genome upon over-expression of TgHU (67) together with the plDNA-specific interaction and DNA condensation properties of PfHU described here are indicative of its significance in the process of apicoplast DNA replication and organellar division.

ACKNOWLEDGEMENTS

We thank Dr Samir Sawant and Amol Ranjan for help with confocal microscopy, Anita Mann for AFM analysis, Ashutosh and Dr Amogh Sahasrabuddhe for helpful discussion and J.P. Srivastava for technical assistance. E.V.S.R.R. and R.N. are recipients of research fellowships from the Council of Scientific and Industrial Research and Department of Biotechnology, respectively. This is CDRI communication no. 7456. Funding by the Council of Scientific and Industrial research (NWP-0038 and NMITLI grant TLP-0010 to SH) is acknowledged. The Open Access publication charges for this article were waived by Oxford University Press.

Conflict of interest statement. None declared.

REFERENCES

1. Wilson,R.J.M. (Iain) (2002) Progress with parasite plastids. *J. Mol. Biol.*, **319**, 257–274.
2. Foth,B.J. and McFadden,G.I. (2003) The apicoplast: a plastid in *Plasmodium falciparum* and other apicomplexan parasites. *Int. Rev. Cytol.*, **224**, 57–110.
3. Wilson,R.J.M. (Iain) (2005) Parasite plastids: approaching the endgame. *Biol. Rev.*, **80**, 129–153.
4. Fichera,M.E. and Roos,D.S. (1997) A plastid organelle as a drug target in apicomplexan parasites. *Nature*, **390**, 407–409.
5. Gardner,M.J., Williamson,D.H. and Wilson,R.J.M. (1991) A circular DNA molecule in malaria parasites encodes an RNA polymerase like that of prokaryotes and chloroplasts. *Mol. Biochem. Parasitol.*, **44**, 115–124.
6. Chaubey,S., Kumar,A., Singh,D. and Habib,S. (2005) The apicoplast of *Plasmodium falciparum* is translationally active. *Mol. Microbiol.*, **56**, 81–89.
7. Kohler,S., Delwiche,C.F., Denny,P.W., Tilney,L.G., Webster,P., Wilson,R.J.M., Palmer,J.D. and Roos,D.S. (1997) A plastid of probable green algal origin in apicomplexan parasites. *Science*, **275**, 1485–1489.
8. Matsuzaki,M., Kikuchi,T., Kojima,S. and Koroiwa,T. (2001) Large amounts of apicoplast nucleoid DNA and its segregation in *Toxoplasma gondii*. *Protoplasma*, **218**, 180–191.
9. Williamson,D.H., Preiser,P.R., Moore,P.W., McCready,S., Strath,M., Wilson, and Wilson,R.J.M. (Iain) (2002) The plastid DNA of the malaria parasite *Plasmodium falciparum* is replicated by two mechanisms. *Mol. Microbiol.*, **45**, 533–542.
10. Singh,D., Chaubey,S. and Habib,S. (2003) Replication of the *Plasmodium falciparum* apicoplast DNA initiates within the inverted repeat region. *Mol. Biochem. Parasitol.*, **126**, 9–14.
11. Singh,D., Kumar,A., Raghu Ram,E.V.S. and Habib,S. (2005) Multiple replication origins within the inverted repeat region of the *Plasmodium falciparum* apicoplast genome are differentially activated. *Mol. Biochem. Parasitol.*, **139**, 99–106.
12. Striepen,B., Crawford,M., Shaw,M., Tilney,L.D., Seeber,F. and Roos,D.S. (2000) The plastid of *Toxoplasma gondii* is divided by association with the centrosomes. *J. Cell. Biol.*, **151**, 1423–1434.
13. Seow,F., Sato,S., Janssen,C.S., Riehle,M.O., Mukhopadhyay,A., Phillips,R.S., Wilson,R.J.M. (Iain) and Barrett,M.P. (2005) The plastidic DNA replication enzyme complex of *Plasmodium falciparum*. *Mol. Biochem. Parasitol.*, **141**, 145–153.
14. Dar,M.A., Sharma,A., Mondal,N. and Dhar,S.K. (2007) Molecular cloning of apicoplast-targeted *Plasmodium falciparum* DNA gyrase genes: unique intrinsic ATPase activity and ATP-independent dimerization of PfGyrB subunit. *Euk. Cell*, **6**, 398–412.
15. Ram,E.V.S.R., Kumar,A., Biswas,S., Kumar,A., Chaubey,S., Siddiqi,M.I. and Habib,S. (2007) Nuclear *gyrB* encodes a functional subunit of the *Plasmodium falciparum* gyrase that is involved in apicoplast DNA replication. *Mol. Biochem. Parasitol.*, **154**, 30–39.
16. Varshavsky,A.J., Nedospasov,S.A., Bakayev,V.V., Bakayeva,T.G. and Georgiev,G.P. (1977) Histone-like proteins in the purified *Escherichia coli* deoxyribonucleoprotein. *Nucleic Acids Res.*, **4**, 2725–2745.
17. Drlica,K. and Rouviere-Yaniv,J. (1987) Histone-like proteins of bacteria. *Microbiol. Rev.*, **51**, 301–319.
18. Chan,Y-H. and Wong,A.T.Y. (2007) Concentration-dependent organization of DNA by the dinoflagellate histone-like protein HCc3. *Nucleic Acids Res.*, **35**, 2573–2583.
19. Kobayashi,T., Takahara,M., Miyagishima,S., Kuroiwa,H., Sasaki,N., Ohta,N., Matsuzaki,M. and Kuroiwa,T. (2002) Detection and localization of a chloroplast-encoded HU-like protein that organizes chloroplast nucleoids. *Plant Cell*, **14**, 1579–1589.
20. Christodoulou,E., Rypniewski,W.P. and Vorgias,C.E. (2003) High-resolution X-ray structure of the DNA-binding protein HU from the hyper-thermophilic *Thermotoga maritima* and the determinants of its thermostability. *Extremophiles*, **7**, 111–122.
21. Skarstad,K., Baker,T.A. and Kornberg,A. (1990) Strand separation required for initiation of replication at the chromosome origin of *E. coli* is facilitated by a distant RNA-DNA hybrid. *EMBO J.*, **9**, 2341–2348.
22. Kano,Y., Ogawa,T., Ogura,S., Hiraga,T., Okazaki,T. and Imamoto,F. (1991) Participation of histone-like protein HU and of IHF in minichromosomal maintenance in *Escherichia coli*. *Gene*, **103**, 25–30.
23. Dri,A.M., Moreau,P.L. and Rouviere-Yaniv,J. (1992) Role of the histone-like proteins OsmZ and HU in homologous recombination. *Gene*, **120**, 11–16.
24. Manna,D. and Gowrishankar,J. (1994) Evidence for involvement of protein HU and RpoS in transcription of the osmoresponsive *proU* operon in *Escherichia coli*. *J. Bacteriol.*, **176**, 5378–5384.
25. Kar,S., Choi,E.J., Guo,F., Dimitriadis,E.K., Kotova,S.L. and Adhya,S. (2006) Right-handed DNA supercoiling by an octameric form of histone-like protein HU: modulation of cellular transcription. *J. Biol. Chem.*, **281**, 40144–40153.
26. Kim,J., Yoshimura,S.H., Hizume,K., Ohniwa,R.L., Ishihama,A. and Takeyasu,K. (2004) Fundamental structural units of the *Escherichia coli* nucleoid revealed by atomic force microscopy. *Nucleic Acids Res.*, **32**, 1982–1992.
27. Talukder,A.A., Iwata,A., Nishimura,A., Ueda,S. and Ishihama,A. (1999) Growth phase-dependent variation in protein composition of the *Escherichia coli* nucleoid. *J. Bacteriol.*, **18**, 6361–6370.
28. van Noort,J., Verbrugge,S., Goosen,N., Dekker,C. and Dame,R.T. (2004) Dual architectural roles of HU: Formation of flexible hinges and rigid filaments. *Proc. Natl Acad. Sci. USA*, **101**, 6969–6974.
29. Lambros,C. and Vandenberg,J.P. (1979) Synchronization of *Plasmodium falciparum* erythrocytic stages in culture. *J. Parasitol.*, **65**, 418–420.
30. Baca,A.M. and Hol,W.G. (2000) Overcoming codon bias: a method for high-level over expression of Plasmodium and other AT-rich parasite genes in *Escherichia coli*. *Int. J. Parasitol.*, **30**, 113–118.
31. Ghosh,S. and Grove,A. (2006) The *Deinococcus radiodurans* encoded HU protein has two DNA binding domains. *Biochemistry*, **45**, 1723–1733.
32. Gissot,M., Briquet,S., Refour,P., Boschet,C. and Vaquero,C. (2005) PfMyb1, a *Plasmodium falciparum* transcription factor, is required

for intraerythrocytic growth and controls key genes for cell cycle regulation. *J. Mol. Biol.*, **346**, 29–42.
33. Tonkin,C.J., van Dooren,G.G., Spurck,T.P., Struck,N.S., Good,R.T., Handman,E., Cowman,A.F. and McFadden,G.I. (2004) Localization of organellar proteins in *Plasmodium falciparum* using a novel set of transfection vectors and a new immunofluorescence fixation method. *Mol. Biochem. Parasitol.*, **137**, 13–21.
34. Foth,B.J., Ralph,S.A., Tonkin,C.J., Struck,N.S., Fraunholz,M., Roos,D.S., Cowman,A.F. and McFadden,G.I. (2003) Dissecting apicoplast targeting in the malaria parasite *Plasmodium falciparum*. *Science*, **299**, 705–708.
35. Chan,Y.N., Kwok,A.C.M., Tsang,J.S.H. and Wong,J.T.Y. (2006) Alveolata histone-like proteins have different evolutionary origins. *J. Evol. Biol.*, **19**, 1717–1721.
36. Christodoulou,E., Rypniewski,W.R. and Vorgias,C.E. (2003) High-resolution X-ray structure of the DNA-binding protein HU from the hyperthermophilic *Thermotoga maritima* and the determinants of its thermostability. *Extremophiles*, **7**, 111–122.
37. Burley,S.K. and Petsko,G.A. (1985) Aromatic-aromatic interaction: a mechanism of protein structure stabilization. *Science*, **229**, 23–28.
38. Rice,P.A., Yang,S.W., Mizuuchi,K. and Nash,H.A. (1996) Crystal structure of IHF-DNA complex: a protein induced DNA U-turn. *Cell*, **87**, 1295–1306.
39. Grove,A. and Saavedra,T.C. (2002) The role of surface-exposed lysines in wrapping DNA about the bacterial histone-like protein HU. *Biochemistry*, **41**, 7597–7603.
40. White,S.W., Appelt,K., Wilson,K.S. and Tanaka,I. (1989) A protein structural motif that bends DNA. *Proteins*, **5**, 281–288.
41. Linding,R., Jensen,L.J., Diella,F., Bork,P., Gibson,T.J. and Russell,R.B. (2003) Protein disorder prediction: implication for structural proteomics. *Structure (Camb)*, **11**, 1453–1459.
42. Swinger,K.K., Lemberg,K.M., Zhang,Y. and Rice,P.A. (2003) Flexible DNA bending in HU-DNA cocrystal structures. *EMBO J.*, **22**, 3749–3760.
43. Jia,X., Grove,A., Ivancic,M., Hsu,V.L., Geiduscheck,E.P. and Kearns,D.R. (1996) Structure of the *Bacillus subtilis* phage SPO1-encoded type II DNA-binding protein TF1 in solution. *J. Mol. Biol.*, **263**, 259–268.
44. Boelens,R., Vis,H., Vorgias,C.E., Wilson,K.S. and Kaptein,R. (1996) Structure and dynamics of the DNA-binding protein HU from *Bacillus stearothermophilus* by NMR spectroscopy. *Biopolymers*, **40**, 553–559.
45. Williamson,D.H., Preiser,P.R., Wilson, and Wilson,R.J.M. (Iain) (1996) Organelle DNAs: the bit players in malaria parasite DNA replication. *Parasitol. Today*, **12**, 357–362.
46. Mazumdar,J., Wilson,E.H., Masek,K., Hunter,C.A. and Striepen,B. (2006) Apicoplast fatty acid synthesis is essential for organelle biogenesis and parasite survival in *Toxoplasma gondii*. *Proc. Natl Acad. Sci. USA*, **103**, 13192–13197.
47. Ghosh,S. and Grove,A. (2004) Histone-like protein HU from *Deinococcus radiodurans* binds preferentially to four-way DNA junctions. *J. Mol. Biol.*, **337**, 561–571.
48. Hodges-Garcia,Y., Hagerman,P. and Pettijohn,D. (1989) DNA ring closure mediated by protein HU. *J. Biol. Chem.*, **264**, 14621–14623.
49. Kamau,E., Tsihlis,N.D., Simmons,L.A. and Grove,A. (2005) Surface salt bridges modulate the DNA site size of bacterial histone-like HU proteins. *Biochem. J.*, **390**, 49–55.
50. Miao,J., Fan,Q., Cui,L., Li,J., Li,J. and Cui,L. (2006) The malaria parasite Plasmodium falciparum histones: organization, expression, and acetylation. *Gene*, **369**, 53–65.
51. Chandra,B.R., Olivieri,A., Silvestrini,F., Alano,P. and Shrama,A. (2005) Biochemical characterization of the two nucleosome assembly proteins from *Plasmodium falciparum*. *Mol. Biochem. Parasitol.*, **142**, 237–247.
52. Diffley,J.F.X. and Stillman,B. (1991) A close relative of the nuclear, chromosomal high mobility group protein HMG1 in yeast mitochondria. *Proc. Natl Acad. Sci. USA*, **88**, 7864–7868.
53. Grove,A. and Lim,L. (2001) High-affinity DNA binding of HU protein from the hyperthermophile *Thermotoga maritima*. *J. Mol. Biol.*, **311**, 491–502.
54. Lee,E.C., Hales,L.M., Gumport,R.I. and Gardner,J.F. (1992) The isolation and characterization of mutants of the integration host factor (IHF) of *Escherichia coli* with altered, expanded DNA-binding specificities. *EMBO J.*, **11**, 305–313.
55. Rice,P.A., Yang,S., Mizuuchi,K. and Nash,H.A. (1996) Crystal structure of an IHF-DNA complex: a protein induced DNA U turn. *Cell*, **87**, 1295–1306.
56. Swinger,K.K., Lemberg,K.M., Zhang,Y. and Rice,P.A. (2003) Flexible DNA bending in HU-DNA cocrystal structures. *EMBO J.*, **22**, 3749–3760.
57. Swinger,K.K. and Rice,P.A. (2004) IHF and HU: flexible architects of bent DNA. *Curr. Opin. Struct. Biol.*, **14**, 28–35.
58. Grove,A. (2003) Surface salt bridges modulate DNA wrapping by the type II DNA-binding protein TF1. *Biochemistry*, **42**, 8739–8747.
59. Feng,Z.P., Zhang,X., Han,P., Arora,N., Anders,R.F. and Norton,R.S. (2006) Abundance of intrinsically unstructured proteins in *Plasmodium falciparum* and other apicomplexan parasite proteomes. *Mol. Biochem. Parasitol.*, **150**, 256–267.
60. Shi,W.-X. and Larson,R.G. (2005) Atomic Force Microscopic study of aggregation of RecA-DNA nucleoprotein filaments into left-handed supercoiled bundles. *Nano Lett.*, **5**, 2476–2481.
61. Dame,R.T., Wyman,C. and Goosen,N. (2000) H-NS mediated compaction of DNA visualized by atomic force microscopy. *Nucleic Acids Res.*, **28**, 3504–3510.
62. Waller,R.F., Keeling,P.J., vanDooren,G.G. and McFadden,G.I. (2003) Comment on 'A green algal apicoplast ancestor'. *Science*, **301**, 49.
63. Funes,S., Reyer-Prieto,A., Perez-Martinez,X. and Gonzalez-Halphen,D. (2004) On the evolutionary origins of apicoplasts: revsisiting the rhodophyte vs. chlorophyte controversy. *Microbes Infect.*, **6**, 305–311.
64. Sato,N., Terasawa,K., Miyajima,K. and Kabeya,Y. (2003) Organization, developmental dynamics and evolution of plastid nucleoids. *Int. Rev. Cytol.*, **232**, 217–262.
65. Arenas,A.F., Escobar,A.J.G. and Gomez-Marin,J.E. (2007) Evolutionary origin of the protozoan parasites histone-like proteins (HU). *In Silico Biol.*, **8**, 0002.
66. Chodavarapu,S., Felczak,M.M., Yaniv,J.R. and Kaguni,J.M. (2008) *Escherichia coli* DNA interacts with HU in initiation at the *E.coli* replication origin. *Mol. Microbiol.*, **67**, 781–792.
67. Vaishnava,S. and Striepen,B. (2006) The cell biology of secondary endosymbiosis- how parasites build, divide and segregate the apicoplast. *Mol. Microbiol.*, **61**, 1380–1387.